CONF-741029--97

MASTER

NOTICE
This report was prepared as an account of work sponsored by the United States Government. Neither the United States nor the United States Energy Research and Development Administration, nor any of their employees, nor any of their contractors, subcontractors, or their employees, makes any warranty, express or implied, or assumes any legal liability or responsibility for the accuracy, completeness or usefulness of any information, apparatus, product or process disclosed, or represents that its use would not infringe privately owned rights.

By acceptance of this article, the publisher and/or recipient acknowledges the U.S. Government's right to retain a non-exclusive, royalty-free license in and to any copyright covering the article.

DESIGN OF FORCE-COOLED CONDUCTORS FOR LARGE FUSION MAGNETS*

L. Dresner and J. W. Lue
Fusion Energy Division
Oak Ridge National Laboratory
Oak Ridge, Tennessee 37830

Abstract

Conductors cooled by supercritical helium in forced convection are under active consideration for large toroidal fusion magnets. One of the central problems in designing such force cooled conductors is to maintain an adequate stability margin while keeping the pumping power tolerably low. A method has been developed for minimizing the pumping power for fixed stability by optimally choosing the matrix-to-superconductor and the metal-to-helium ratios. Such optimized conductors reduce pumping power requirements for fusion size magnets to acceptable limits. Furthermore, the mass flow and hence pumping losses can be varied through a magnet according to the local magnetic field and magnitude of desired stability margin. Force cooled conductors give flexibility in operation, permitting, for example, higher fields to be obtained than originally intended by lowering the bath temperature or increasing the pumping power or both. This flexibility is only available if the pumping power is low to begin with. Scaling laws for the pumping requirement and stability margin as functions of operating current density, number of strands and such physical parameters as stabilizer resistivity and critical current density, have been proved. Numerical examples will be given for design of conductors intended for use in large toroidal fusion magnet systems.

1. Introduction

One type of conductor under consideration for tokamak toroidal field (TF) magnets is a cable-in-conduit cooled by supercritical helium in forced convection. The main problem in designing such force-cooled conductors (FCC) is to maintain adequate stability while keeping the pumping power tolerably low.

The transit time of the helium through a coil is many minutes. Since recovery of the conductor from a thermomechanical perturbation takes on the order of tens of milliseconds, for purposes of calculation, the inventory of helium available to promote recovery is finite. This means that a large enough perturbation will quench the conductor. We can then judge the stability of an fcc by the maximum perturbation of some specified type against which the conductor is stable, i.e., can still return to the superconducting state. The simplest type of perturbation is a sudden, uniform heat input over the entire length of the conductor. We call the maximum, sudden, uniform heat input per unit volume of metal ΔH the "stability margin." We emphasize that this definition of the stability margin has been chosen not because we believe a sudden, uniform heat input is likely to occur, but (i) it provides a basis for comparison of different conductors, (ii) it is relatively easy to calculate, and (iii) it is a lower limit to the specific energy input of any perturbation, i.e., the conductor is stable to any perturbation when the specific energy input is less than ΔH.

2. Design Procedures

In an earlier paper,[1] a systematic method was developed for finding the fcc with a fixed stability margin that consumes the least pumping power. The stability margin is determined by ten data: T_b, B, I, ρ, J_c, A, P, h_b, f, and f_{co}. (There is an alphabetic list of symbols and their definitions at the end of this article.) We can reduce these ten to eight as follows. First, P and h_b always occur in the product Ph_b. Second, for a given arrangement of strands of a given shape, the stability margin of a part of the conductor is the same as that of the whole. This means that if the original conductor is imagined to be composed of two smaller conductors in parallel, each of which has half the number of strands, half the area, and half the cooled perimeter of the original, then each half will have the same stability margin as the original. Thus ΔH can depend only on P/A and on I/A = J, the overall current density. Our original list of ten arguments can thus be reduced to the following eight: T_b, B, ρ, J, J_c; Ph_b/A; f, f_{co}.

We have separated the eight independent variables into three groups of five, one, and two, respectively. These will aid in describing our design procedure. It consists of the following six steps:

Step 1 Values of T_b, B, ρ, J, and J_c are fixed.

Step 2 For several values of Ph_b/A, we maximize ΔH by variation of f and f_{co}. (It is shown in Ref. 1 that such a maximum always exists.)

Step 3 We plot $(\Delta H)_{max}$ and the corresponding values of f and f_{co} against Ph_b/A.

Step 4 We choose some suitable stability margin ΔH and find the corresponding values of Ph_b/A, f, and f_{co} from the plot made in Step 3.

Step 5 Keeping Ph_b/A fixed, we increase P/A and decrease h_b, but only until the Reynolds number Re falls to 5000. A Reynolds number of 5000 should be sufficient to maintain fully developed turbulence. This step has the effect of further reducing the pressure drop and pumping power while maintaining ΔH fixed.

Step 6 We seek a cabling pattern that will conveniently realize the values of f_{co} and P/A found above.

These steps can be made more comprehensible if we note that

$$\text{pumping power per unit volume of conductor} \sim (Ph_b/A)^2\,(Re)^{23/20}, \qquad (1)$$

and

$$\text{pressure drop per unit length of conductor} \sim (Ph_b/A)^{3/2}\,(Re)^{11/20}\,. \qquad (2)$$

These scaling relations can be derived by taking $h_b \sim v^{0.8}\,D^{-0.2}$ (Dittus-Boelter equation) and using Blasius's equation for the friction factor. Steps 1-4 minimize Ph_b/A for a given ΔH, and

*This research sponsored by the Department of Energy under contract with Union Carbide Corporation.

DISTRIBUTION OF THIS DOCUMENT IS UNLIMITED

Step 5 reduces Re to the lowest tolerable value.

The numerical program will not be described here in detail, but a few words will be said about its capabilities and what it takes into account. It can be run either in a case-by-case interative mode using all eight input variables and returning ΔH; or it can perform the maximization of Step 2 automatically. The superconductor can be either NbTi or Nb_3Sn; the matrix can be either Cu or Al. Current sharing is taken into account, as are the temperature variations of the specific heats of matrix and superconductor. Also included is the latent heat of the superconducting-resistive transition in a magnetic field. Heat transfer is described by Giarratano's modified Dittus-Boelter equation.[2] The thermodynamic variables of helium can be chosen to correspond either to constant-pressure or to constant-volume operation.

3. Numerical Examples

3.1 NbTi Magnet

As an example, let us consider the design of a 15-kA NbTi/Cu fcc operating at 4.0 K and 8.0 T using a superconductor the critical current of which is normalized to 5.6×10^6 Am^{-2} at 4.2 K and 8.0 T. Let us strive for a current density over the cable space of 3750 Acm^{-2}. This means a cross-sectional area of 4.0 cm^2. Let us further suppose that the residual resistance ratio of the copper at zero field is 160. At 8.0 T, the resistivity of the copper will be 5.35×10^{-10} ohm m. (Due to the effect of magneto-resistance, values close to this one will be obtained for a wide choice of residual resistance ratios at zero field.)

Figure 1 shows the results of the first five steps of our procedure: ΔH is plotted against pumping

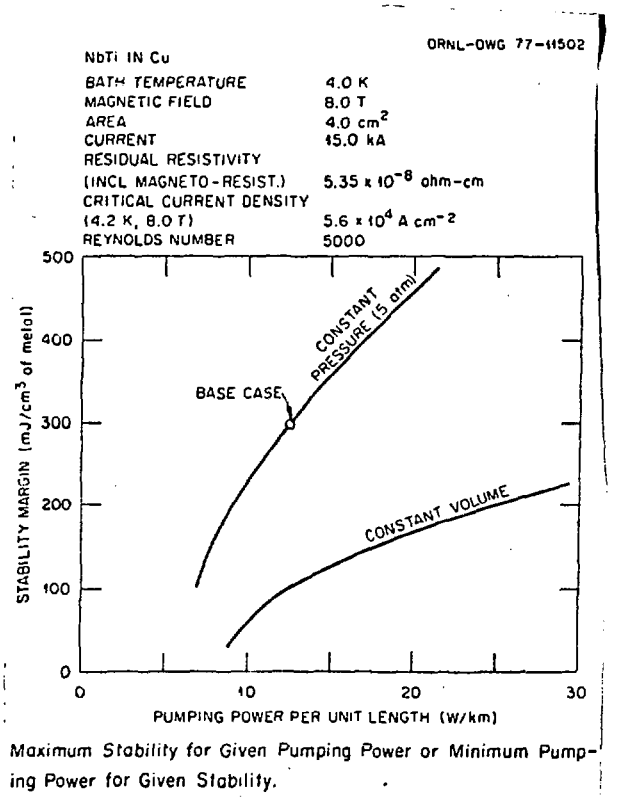

Fig. 1. Results of the first five steps of the design procedure.

power per unit length of the conductor. The Reynolds number has already been reduced to 5000. For all the optimized conductors represented here, f lies between about 0.7 and 0.8, while f_{co} lies between about 0.4 and 0.5. Noteworthy is the much larger stability margin in constant-pressure operation than in constant-volume operation. The difference is due to the larger specific heat of helium at constant pressure than at constant volume. The constant-pressure curve applies to ambient pressures between 3 and 7 atms. ΔH does not depend on pressure because in this pressure range and in the range of temperatures between the bath temperature (4.0 K) and the current sharing threshold (<5.0 K), the specific heat of helium at constant pressure is nearly pressure independent (see Fig. 2). ΔH is not always pressure independent, and later we shall discuss a Nb_3Sn conductor in which ΔH shows a strong dependence on ambient pressure.

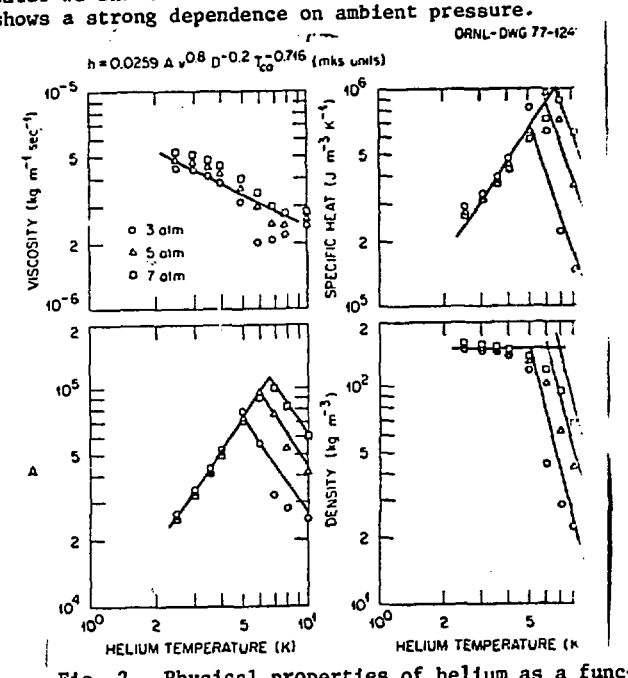

Fig. 2. Physical properties of helium as a function of pressure and temperature. The points are from NBS-631; the lines are fits used in the computer program.

Let us assume constant-pressure operation and choose ΔH = 300 mJ cm^{-3} of metal as an acceptable stability margin. The conductor selected is shown in Fig. 1 as the base case; ΔH = 300 mJ/cm^3 corresponds to a temperature rise to 18 K. This conductor is about 51% metal and 49% helium by volume; the copper-to-superconductor ratio is 3.5. The helium velocity in the interstices is 23 cm sec^{-1} corresponding to a mass flow of 7 g sec^{-1} through the entire 4.0-cm^2 cross section. The cooled perimeter is 1.45 m, the pumping power 12 W km^{-1}, and the pressure drop 0.27 atm/100.

It should be remembered that the pumping power and the pressure drop have been calculated using smooth tube friction factors appropriate to the given hydraulic diameter. Recent experiments by Hoenig[3] have shown that in cables wound of twisted triples, the friction factor is about three times that in a smooth tube. To get a more realistic impression of the performance of the base-case conductor, we ought to multiply the pumping power and pressure drop by a factor of three. Since the pumping power is dissipated as heat in the helium, it must be gotten rid of by refrigeration. To calculate the room-temperature

work required to do this, we multiply by 500; thus we get a refrigeration work load of 12 X 3 X 500 = 1.8 X 10^4 W/km of conductor. A typical tokamak TF coil system might contain 250 km of conductor altogether, so that the total refrigeration work load due to pumping would be 4.5 MW.

3.2 Cabling Patterns

Next we look for a cabling pattern by which we can realize the specifications calculated so far. We discuss two possibilities here, one needing little compaction and the other needing considerable compaction. In both cases, the basic unit is a soldered triple of composite wires each of which is 0.46 mm in diameter. Because of the soldering, the interstice is assumed to be filled with solder, and the part of the surface inside it is assumed unavailable for heat transfer. One cabling pattern is to wind these triples in layers around a central core. Alternate layers twist in opposite directions and therefore do not interpenetrate; the triples are also twisted so that adjacent triples do not interpenetrate. To attain the required cooled perimeter, we shall need about 1200 such wires. Eleven layers around the central core will contain about 405 triples (the exact number depends on the twist pitch). The crosssectional area is 4.0 cm^2 as required, and the helium volume fraction is 50% at the beginning. For this reason, this conductor will require only slight compaction. The cabling pattern is shown in the bottom part of Fig. 3.

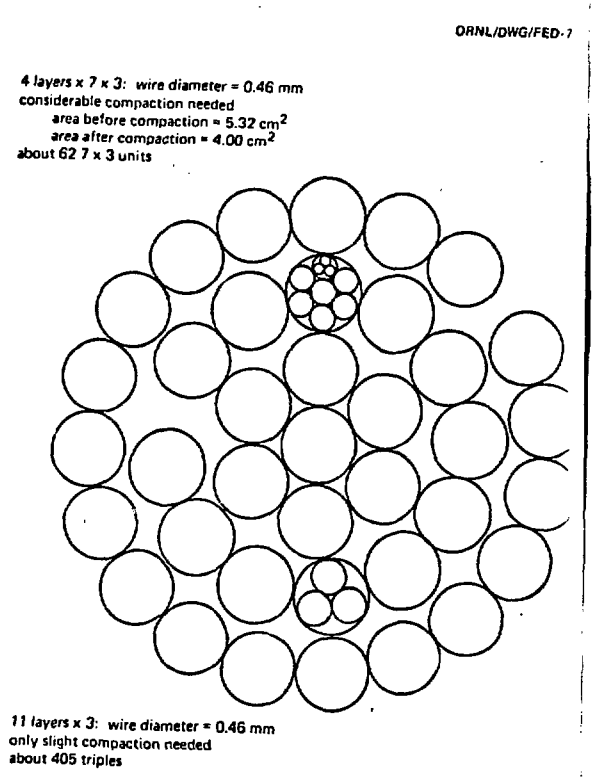

Fig. 3. Two cabling patterns by which the NbTi/Cu conductor found using our design procedure may be realized.

The second cabling pattern uses wires of the same size, but the basic unit is a single layer of triples wound around a central triple (7 X 3 unit). Fifty-eight such units will provide the requisite number of wires; four layers around a central core will contain about 62 such units. Uncompacted, such an arrangement will have a helium fraction of 62% and a cross-sectional area of 5.32 cm^2. Compaction to 4.0 cm^2 will bring the helium fraction to 50%. This cabling pattern is shown in the top part of Fig. 3.

3.3 Nb_3Sn Magnet

The next problem is related to the first in that again we design a 15-kA, 4.0-cm^2 conductor. This time the conductor is composed of Nb_3Sn/CuSn/Cu. We choose as our operating point a helium temperature of 6.0 K, a helium pressure of 7.0 atm, and a magnetic field of 12.0 T. Because the stability margin will depend on pressure, it is necessary to specify the helium pressure in this example, whereas in the first example it was not. The resistivity of the copper in a 12-T field is 6.79 X 10^{-10} ohm m (RRR = 160, as before). The critical current density of the Nb_3Sn is taken to be 1.2 X 10^9 A m^{-2} at 12 T and 4.2 K. Finally, the CuSh/Nb_3Sn volume ratio is fixed at 3.

After the first five steps of our design procedure, we again arrive at a curve of ΔH versus pumping power for constant-pressure operation. This curve has a fairly pronounced "knee" in it, the bend in the "knee" being located near the point ΔH = 365 $mJcm^{-3}$ and a pumping power of 6.0 Wkm^{-1}. The corresponding pressure drop is 0.19 atm/100 m. The conductor is 58% metal, 42% helium by volume; the metal is 50% copper and 50% CuSn + Nb_3Sn by volume. The cooled perimeter is 1.22 m. ΔH = 365 mJ/cm^3 corresponds to a temperature rise to 20 K for this conductor.

If we examine Fig. 2, we see that the operating point 6.0 K, 7 atm is close to the point at which the specific heat of helium and the heat transfer coefficient have reached their maxima. at 7 atm, the specific heat and heat transfer coefficient should have nearly reached their maximum values in the range of helium temperatures between the bath temperature (6.0 K) and the current sharing threshold (<7.0 K). But if the ambient pressure of the helium were less than 7 atm, say 5 atm, then the specific heat and heat transfer coefficient would be considerably reduced. Consequently, we expect a decrease in stability margin with decreasing pressure for this conductor. The results of detailed calculations are shown in Table 1.

Table 1. Dependence of stability margin on ambient pressure for base-case Nb_3Sn conductor

Pressure (atm)	Stability margin (mJ/cm^3-metal)	Temperature (K)
7	365	20
6	290	19
5	150	16
4	26	9

4. Scaling Relationship

The flowing helium in a force-cooled magnet fulfills two functions: it is a heat sink for the conductor, and it transfers the heat away from the conductor. In a large magnet, the helium is stagnant as far as the heat sink function is concerned. This has been the basis of our zero-dimensional analysis. The ultimate cooling power is limited by the enthalpy change from the initial helium bath temperature to the current sharing temperature. Per unit conductor volume, it is given by

$$\Delta H_G = [H_{co}(T_{cs}) - H_{co}(T_b)] + [H_{He}(T_{cs}) - H_{He}(T_b)] \frac{A_{He}}{A_{co}} . \quad (3)$$

Since the enthalpy of helium is about two orders of magnitude higher than that of the conductor at helium temperatures, the second term dominates.

The heat transfer coefficient of helium varies as the flow changes. This determines the recovery time and thus the stability margin. As is stated in Sect. 2, the heat transfer coefficient depends on the velocity and hydraulic diameter as

$$h_b \sim v^{0.8} D^{-0.2} . \quad (4)$$

Assuming smooth tube friction factors, one also finds the following relationship between the pumping power and the flow velocity.

$$P_p \sim \frac{A_{He}}{D^{1.25}} v^{2.75} . \quad (5)$$

The functional dependence of ΔH on P_p for the two base cases derived in Sect. 3 is shown in Fig. 4. It is interesting to note that ΔH changes sharply only in a range of P_p about an order of magnitude wide. At very high pumping power the heat transfer coefficient will be high enough to transfer heat from conductor to helium immediately. The amount of heat that the conductor can take is limited by the helium inventory. The stability margin approaches that given by Eq. (3). The kink in each of the curves

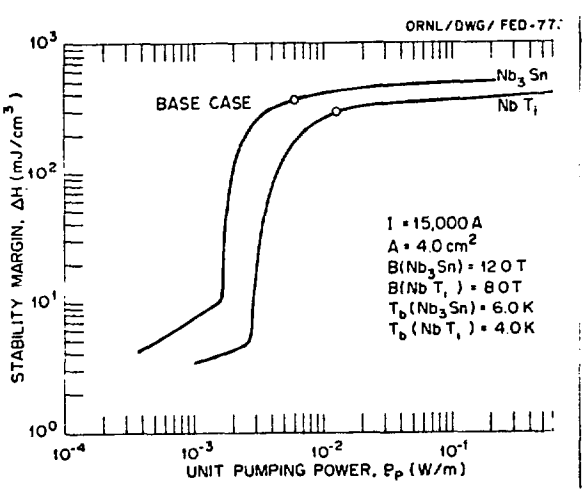

Fig. 4. Stability margin versus pumping power for the two base-case conductors.

corresponds to the conductor being heated to T_c initially. For initial thermal disturbances less than this value, the conductor does not go completely normal. This region is not of practical interest.

Above the kink all current flows in the substrate initially. Joule heating becomes a constant. A small increase in h_b of P_p will allow a substantial increase in ΔH. Hence, between the shoulder and kink of the curve, ΔH is very sensitive to P_p. The recovery capability of a conductor in this region can be inferred by comparison of the heat transfer and the power density of joule heating in the conductor

$$Ph_b (T_o - T_b) : \frac{I^2 \rho}{f A_{co}} . \quad (6)$$

For a given initial conductor temperature, T_o, corresponding to a stability margin ΔH, one can find the parametric scaling by holding

$$\frac{I^2 \rho}{Ph_b} = \text{constant}. \quad (7)$$

4.1 J-Dependence

One interesting question is what will be the changes in the stability limits and pumping power requirements by running a conductor at different current densities. With a linear relationship between the superconductor critical current density and the temperature, one finds from Eq. (3) that

$$\Delta H_G \sim (1 - \frac{J}{J_c}) , \quad (8)$$

the ultimate gradual heat input limit increases linearly as the current density decreases. In the range of helium flow where the stability margin depends strongly on the heat transfer coefficient, Eqs. (4), (5), and (7) give

$$P_p \sim J^{6.88} . \quad (9)$$

The pumping power requirement is a very strong function of current density. Thus, reducing operating current density not only increases the ultimate heat capacity but also substantially reduces the required pumping power. Numerical examples of this scaling relationship for a 20-mm-ID conductor are shown in Fig. 5. One finds that Eq. (8) applies to the vertical shifts at the right and Eq. (9) applies to regions between the shoulder and the kink.

4.2 ρ Dependence

Radiation damage to the conductor of a fusion magnet will gradually increase the resistivity of the substrate. Thus the stability of the magnet will be degraded. One can warm up the magnet periodically to anneal the conductor or degrade the magnet by operating at a reduced current in accordance with $I \sim 1/\sqrt{\rho}$ to maintain the same stability. The force-flow cooling scheme offers another choice. From Eqs. (4), (5), and (7) again one finds

$$P_p \sim \rho^{3.44} . \quad (10)$$

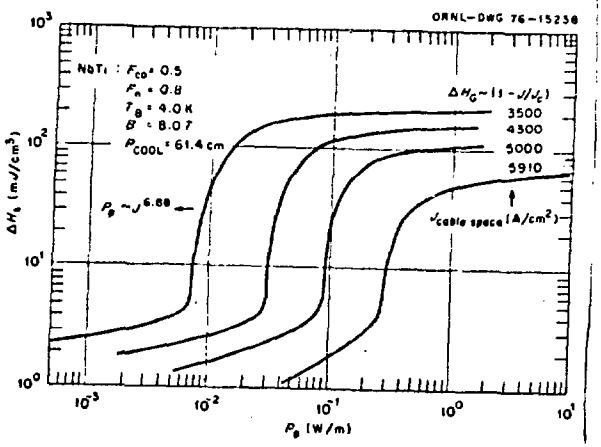

Fig. 5. Current density dependence of the stability margin and pumping power. The constant-volume specific heat of helium was used, A = 3.14 cm².

Thus by increasing the pumping power in this proportion, the same stability margin can also be maintained. The degradation of ρ, however, will not affect ΔH_G.

4.3 Strand Number Dependence

As is noted in Sect. 2, P and h_b always occur in the product Ph_b. Lower h_b and thus lower pumping power can be realized by increasing P or having a large number of strands. This, however, cannot go too far because of possible difficulties in manufacture and possible flow instability. Since P is roughly proportional to the square root of the number of strands, $\sqrt{N_s}$, one finds from Eqs. (4), (5), and (7) that

$$P_p \sim N_s^{-1.44} . \qquad (11)$$

4.4 B- and T-Dependence

No simple scaling relationships, however, can be found for the dependence on field and temperature. The field, the helium temperature, the critical current density, and the critical temperature enter in more than one place. Numerical calculation[4] is required for these cases. Table 2 summarizes all the scaling relationships discussed.

5. Other Considerations

5.1 Comparison with MIT Experiment

Experiments on the stability of force-cooled cable conductors have been performed at FBNML-MIT by M. O. Hoenig, et al.[5] As a test of our computer analysis, we calculated the stability margin of the conductor for different operating currents at various fields. An example of the comparison between this analysis and the data is shown in Fig. 6. The experiment was performed on a 19-strand triplex cable in a 10.2 mm ID aluminum conduit. The initial heat input was supplied by eddy current heating over a period of 20 msec, while the analysis assumed that heat was added instantaneously. Stability margins at different I/I_c are plotted against helium velocity.

Table 2. Scaling relationships

Physical entity	Scaling factor
Ultimate gradual heat input limit	$H_{He}(T_{cs}) - H_{He}(T_b)$
ΔH_G(mJ/cm³-cond)	A_{He}/A_{co}
	$1 - J/J_c$
	S_{He}
	$T_c - T_b$
Unit pumping power	A_{He}
P_p(w/m)	$v^{2.75}$
	$J^{6.88}$
	$\rho^{3.44}$
	$p^{-2.88}$
	$N_s^{-1.44}$

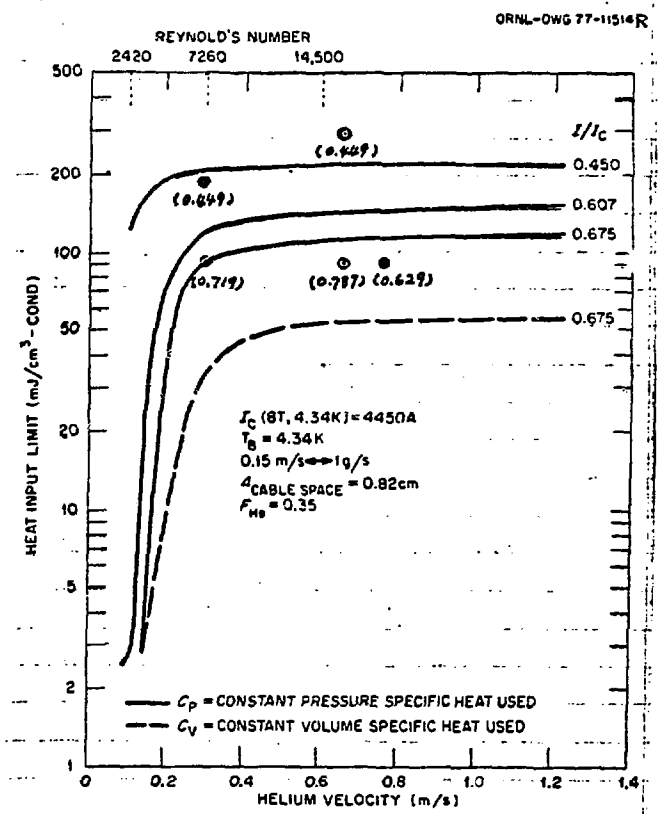

Fig. 6. Comparison of the present analysis and the FBNML-MIT experiment. The number in the parenthesis is the experimental I/I_c.

There is good agreement between the analysis and data for the gradual heat input limit. On the other hand, the experimental data on the stability margin do not clearly test the rapid fall off at low velocities predicted by the analysis. Note also that the data confirm the more advantageous constant-pressure mode of operation.

5.2 Nonuniform Cooling

One concern about the cable-in-conduit conductor is that the interstices of the cable where the helium flows may not be uniformly distributed. Furthermore as the conductor is energized in a magnet, the Lorentz force may push the cable toward one side, thus reducing the cooling of the strands. To treat these problems in the zero-dimensional analysis, we consider the latter case of the cable being shuffled to one side with a big void left behind. The helium flowing through this void is considered to be wasted insofar as its heat transfer function is concerned.

The conductor with the depleted helium was analyzed as usual first. Namely, the flow velocity, v, and the pressure drop, dp/dx, required for a given stability margin were calculated. Since the big void and the remaining cooling channels have parallel flow, dp/dx is the same for all the channels. One finds that

$$v_i \sim D_i^{0.71} \quad . \tag{12}$$

The larger the void, the higher the helium flow and the larger the waste. The total pumping power requirement is calculated by the summation

$$P_p = (\sum_i A_{He_i} v_i)\ dp/dx \quad . \tag{13}$$

Examples of this treatment for an extreme case of 1/8 of the cable space being opened are shown in Fig. 7. Note that the contribution of the helium flowing through the void to the ultimate heat capacity still exists and was added to the curves above the shoulder. It is seen that depending on how badly the compacted part is smashed, i.e., how much the cooled perimeter is reduced, a factor of 2 to 3 increase in pumping power is required to regain the same stability margin. It is judged that nonuniform cooling in the proposed cable will not cause any alarming difficulties.

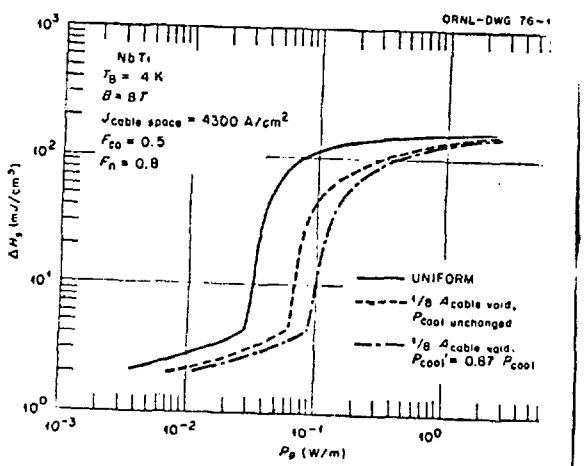

Fig. 7. Effects of nonuniform cooling due to strands being pushed to one side. Extreme case of 1/8 of the cable space being opened is shown.

5.3 Producing Higher Fields

The force-flow cooling scheme offers very valuable flexibility in that it can be operated at different temperatures and pumping speeds. The inlet helium temperature and pressure is set by the refrigerator and the pump, both of which can be outside the magnet. As is well known, lower coolant temperature will increase superconductor critical current density. A superconducting magnet can presumably produce higher fields at lower operating temperatures. The engineering complexity of maintaining lower temperature and the uncertainty of the magnet stability at subatmospheric pressures for a pool-boiling cooled magnet are big obstacles, but this will not be the case in a force-flow system.

Assuming the magnet structure has enough safety margin, we consider ways of achieving higher fields in a given magnet with no sacrifice in the stability margin. For the same magnet to produce a higher field, a higher current density is required. At higher fields, the magnetoresistance of the stabilizer (Cu) increases. As is discussed in Sect. 4, the stability margins and the required pumping powers depend on the current density, field, resistivity, and the helium temperature in a complicated way. First, the helium temperature to maintain the same ultimate heat capacity was determined. The sudden heat input limit as a function of the pumping power was then calculated for this particular temperature and field. Figure 8 shows the results of one of these calculations. In order to maintain the same stability margin at higher fields, lower helium temperatures and higher pumping powers are required. Selecting the stability margin as half of the ultimate gradual heat input limit, $\Delta H = (1/2)\ \Delta H_G$, the results are summarized in Table 3. Because of the different helium bath temperatures, the Carnot factor, $(T_r - T_b)/T_b$, was included in calculating the relative pumping power shown in the last column. Note that in this calculation, the constant-volume specific heat of helium was used.

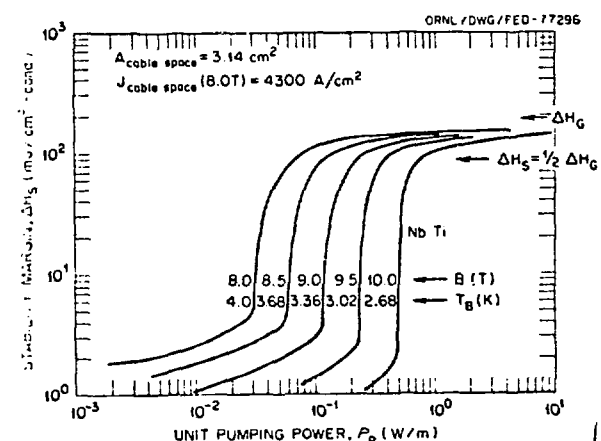

Fig. 8. Operating temperature and pumping power requirement to produce higher magnetic fields in a given magnet.

Table 3. Operating temperature and pumping power for higher fields

B (T)	J (A/cm^2)	T_b [a] (K)	$[P_p (\frac{T_r - T_b}{T_b})]_R$ [b]
8.0	4300	4.0	1.0
8.5	4569	3.68	1.8
9.0	4838	3.36	4.0
9.5	5106	3.02	7.4
10.0	5913	2.68	16.4

[a] Required bath temperature for obtaining ΔH_G = 173 mJ/cm^3.

[b] For $\Delta H = 1/2\ \Delta H_G$ and relative to B = 8.0 T field output.

Symbols

A = total area within the conduit (m^2)

A_{co} = conductor (metal) area (m^2)

A_{He} = helium area (m^2)

B = magnetic field (T)

D = hydraulic diameter (m)

f = volume fraction of copper in metal

f_{co} = volume fraction of metal inside conduit

h_b = heat transfer coefficient when metal temperature is infinitesimally higher than helium temperature ($Wm^{-2}K^{-1}$)

ΔH = stability margin ($mJ\ cm^{-3}$)

ΔH_G = ultimate gradual heat input limit ($mJ\ cm^{-3}$)

H_{He} = enthalpy of helium

H_{co} = enthalpy of metal ($J\ m^{-3}$)

I = transport current (A)

J = overall current density (Am^{-2})

J_c = critical current density of superconductor (Am^{-2})

N_s = number of strands

P = cooled perimeter (m)

Re = Reynolds number

T_b = helium bath temperature (K)

T_c = critical temperature (K)

T_{cs} = current sharing threshold (K)

T_o = initial metal temperature (K)

T_r = room temperature (K)

v = helium velocity in the interstices ($m\ sec^{-1}$)

ρ = matrix resistivity (including magneto resistivity, Ω-m)

References

1. Lawrence Dresner, *IEEE Transactions on Magnetics*, Vol MAG-13, No. 1, pp. 670-72, (1977).
2. P. J. Giarratano, V. Arp, and R. V. Smith, *Cryogenics* 11, 385 (1971).
3. M. O. Hoenig, Y. Iwasa, D. B. Montgomery, and A. Bejan, "Supercritical Helium Cooled, Cabled, Superconducting Hollow Conductors for Large High Field Magnets," 6th Intl. Cryogenic Engineering Conference, May 11-14, 1976, Grenoble, France.
4. J. W. Lue and J. N. Luton, *IEEE Transactions on Magnetics*, Vol. MAG-13, No. 1, pp. 601-04 (1977).
5. M. O. Hoenig, J. W. Lue, and D. B. Montgomery, "Force Cooled Cabled Superconductors," paper presented at the 6th International Conference on Magnet Technology, Bratislava, Czechoslovakia, August 29 - September 2, 1977.